LOCAL DAMAGE IN A 5 – HARNESS SATIN WEAVE COMPOSITE UNDER STATIC TENSION: PART I - EXPERIMENTAL ANALYSIS

S. Daggumati [a*], *I. De Baere*[a] , *W. Van Paepegem*[a], *J. Degrieck*[a], *J. Xu*[b], *S.V. Lomov*[b], *I. Verpoest*[b]

[a]*Ghent University, Dept. of Materials Science and Engineering, Sint-Pietersnieuwstraat 41, 9000 Gent, Belgium*

[b]*Katholieke Universiteit Leuven, Department of Metallurgy and Materials Engineering, Kasteelpark Arenberg 44, B-3001 Leuven, Belgium*

ABSTRACT

This paper presents an experimental damage analysis of a 5-harness satin weave carbon-PPS (PolyPhenylene Sulphide) composite under uni-axial static tensile load. In order to understand the local damage behaviour, tensile tests were performed and accompanied by acoustic emission (AE) and microscopic analysis of the composite specimen. These tests enable us to detect the damage initiation stress as well as the damage initiation location in the composite. Microscopic observation of the tested composite laminates allowed the characterization of the sequence of intra-yarn transverse damage (perpendicular to the load direction) occurrence at different locations in the laminate, starting from crack initiation to the final failure of the composite.

---

*Corresponding author. Tel.: +32 92 64 33 17; fax: +32 92 64 35 87.

E-mail address: Subbareddy.Daggumati@ugent.be

The earliest crack events occurred inside the laminate middle layers, followed by the damage on the traction free surface. It is observed that the initiation of the transverse crack, the location of the crack in the weft yarn cross-section (centre / near the edges) is affected by the relative position of the ply in the laminate (local nesting configuration). The first part of this paper deals with the experimental characterization of sequential damage in a 5-harness satin weave composite. Part II deals with the meso-FE modeling of damage using a satin weave unit cell, and the correlation between experimental and numerical results.

Keywords: Textile composite, Transverse cracking, Acoustic emission, Multiscale modeling, Weft yarn damage

1. Introduction

Damage accumulation in textile composites is a complicated process, and development begins on the micro scale with the fibre matrix debonding, the matrix cracking and the fibre failure (the micro scale defines the arrangement of fibres in an impregnated yarn or fibrous ply). On the meso scale, damage develops by intra-yarn cracking and delaminations (the meso scale defines the internal structure of the reinforcement, variation of the fibre direction and the fibre volume fraction inside the yarns and the fibrous plies). Finally, the macro failure of the composite is characterized by dense cracking, intersection of several small cracks (crack conjunction) and fibre rupture [1] (the macro scale defines the three-dimensional geometry of the composite part and the distribution of local reinforcement properties).

Starting from the micro scale, Figure 1 schematically depicts the weft yarn damage that is affected by the restriction of local ply deformation caused by the surrounding layers. The influence of local constraints is manifested by a change in the weft yarn crack location (edge / centre) based on the location of the chosen ply in the laminate (inner / surface).

In order to obtain comprehensive knowledge of the damage phenomena occurring in textile composites, it is necessary to understand the factors that contribute to the damage at different length scales. Apart from the natural variability in yarn spacing and its dimensions, the unit cells of textile reinforcement are theoretically the same. However, parameters such as the fibre orientation, localized fibre spacing and packing often exhibit a wide statistical variation when evaluated on the micro scale in a processed composite. Therefore, some localized micro volumes are stressed more than others. The stress inhomogeneity is further enhanced by the inhomogeneity of the elastic properties of the composite constituents. The inhomogeneity of the stress field, coupled with the inhomogeneity of the strength properties of the reinforcing elements, the matrix and the interface, lead to the gradual damage development in composites [2]. Moreover, the micro scale stress-strain state defines the number of transverse cracks in a particular yarn and how they are placed over its entire cross-section [3].

In addition to the micro scale parameters mentioned above, at the ply level (meso scale), geometrical parameters such as the yarn crimp and the variations in intra-yarn volume fraction can contribute to the stochastic nature of the stress concentration in the micro volumes [4, 5]. Finally on the scale of laminate, in the textile composite, different layers

have different yarn nesting patterns. The nesting conditions of the particular laminate are defined by the (random) shifting of its layers during the manufacturing process. Hence, the stress-strain state inside the ply (as in the micro volumes) depends on the placement of ply inside the laminate [6-8]. The above mentioned parameters of the textile composites at various hierarchical levels can lead to different damage initiation conditions, different patterns of progressive damage in the chosen ply of a laminate. In general, micro scale damage initiation in a textile composite is not only affected by the stochastic micro level geometrical variables, but also by the meso and laminate level geometrical parameters.

A combination of different experimental techniques is used in the current study to understand the detailed damage phenomena and the damage history. Damage initiation is detected using the acoustic emission (AE) technique during the tensile test. AE provides the damage initiation threshold and the critical stresses of the composite. In order to detect the location of the damage, microscopic analysis is used. The above mentioned methodology has been proposed by many researchers [9-11] to study the damage initiation and propagation in textile composites. From the microscopic images captured during the tensile test, the major damage observed in the satin weave composite is weft yarn cracking before the final failure of the laminate. Based on the microscopic images, apart from the detection of damage initiation stress and locations, a novel procedure is introduced to interpret the layer-wise sequential damage at different locations in the laminate. The aim of using this technique is to provide the information regarding the history of the weft yarn transverse damage in different layers of the laminate. This then

also provides information on the influence of adjacent layers (internal yarn nesting) on the meso damage behavior of a local ply. Finally, the correlation between AE event data and the microscopic crack density provided confidence in the interpretation of the complex damage behavior.

2. The mechanical testing procedure and the material used

Tensile tests on the composite specimens were performed using a standard Instron machine (Instron 4505, test speed 1 mm/min). Composite samples used for the tensile tests were prepared according to the ASTM standard (width 25mm, gauge length 170mm, thickness 2.5 mm), with the end tabs of the same material (Carbon-PPS). The local strain during the tension test is measured using the digital image correlation technique (LIMESS). At the end of the loading process, the average strain is computed across the entire window of the speckle pattern ($23 \times 37 mm$) used for the full-field strain registration [12]. Along with the LIMESS, the AE measurement and data acquisition system (VALLEN) is used to detect the damage initiation stress, followed by the microscopic analysis of the composite specimens for the inspection of damage locations.

2.1 Acoustic emission

It is important to determine the damage initiation and the critical strains over the stress-strain curve obtained from the tension test on the textile composite specimen. Based on the damage initiation and critical strains observed, the composite fatigue and durability life can be determined [13, 14]. To this end, AE has proven to be a valuable technique for

online damage detection as well as for tracking the damage progression. In general, the characteristic failure mechanisms in fibre reinforced composites are initiated at the micro level and result in a spontaneous release of elastic strain energy, which is dissipated as a wave that propagates from the failure source through the medium [11]. These emitted acoustic events are detected by one of the sensors attached to the composite specimen.

Once the composite test specimen is mounted on the tensile machine, two sensors are attached at the ends of the specimen at a distance of 150mm from each other. Special vacuum grease is used to mount the sensors onto the composite, which will transfer the acoustic events from the composite material to the AE sensors. The complete AE VALLEN system used in the current experiment can be obtained from the VALLEN data manual [15]. Details of the AE equipment used for the event registration are shown in Table 1. At the end of the tensile test, AE signals occurred outside the area between sensors, and the external noise was removed from the entire AE data. The obtained AE output combined with the strain data, results are plotted as a logarithm of cumulative acoustic energy versus tensile strain (Figure 3a). By analyzing the different strain levels in Figure 3a, the critical stress at which damage occurs can be detected [14].

2.2. Microscopic analysis

The AE technique described in the above section provides the damage initiation stress quantitatively, but it can not give any indication of the damage locations. In order to visualize the damage locations, microscopic analysis of the composite specimen is a possible technique [16, 17]. The technique presented in this paper (in later sections) is

based on capturing and performing the qualitative as well as the quantitative analysis of the microscopic images. Quasi - static tensile tests were performed on the polished composite specimen to allow for the microscopic inspection of damage initiation and propagation. In order to visualize the damage, an OLYMPUS AX-70 microscope is used along with the 'cell-D' (www.microscopy.olympus.eu) software for the analysis of the microscopic images that were captured.

2.3. Material

The material under study is a thermo-plastic 5-harness satin weave composite (CD0286 supplied by 'Ten Cate'), which has T300 JB carbon fibres as a reinforcement and PPS as a matrix. The composite laminate is manufactured using the press forming technique, which has eight layers of satin weave fabric with 50:50 weight ratios in the warp and weft directions. The details of the 5-harness satin weave fabric are listed in Table 2.

Due to the sensitivity of the micro scale geometrical parameters on the damage behaviour, there is a special focus on investigating the variation of the local yarn cross-section (which directly controls the fibre packing fraction) at various locations of the laminate (Fig 2a-2d). The yarn dimensions, which were measured in different locations of the laminate, revealed that the 5-harness satin weave weft yarn maintained its elliptical shape, with a major diameter of 1.32 ± 0.17 mm, and the minor diameter varying at around 0.15 ± 0.02 mm. The above measured yarn dimensions with 3000 filaments in a bundle showed a constant packing fraction that is independent of the location of the chosen weft yarn.

3. Results and discussion

3.1. Stress –strain diagram, analysis of AE data

In order to obtain critical strains for the damage analysis, the stress versus strain curve is plotted together with the strain versus acoustic energy (Figure 3a). To show consistency in the event pattern for different samples, the event distribution (in a linear scale) is plotted with the tensile stress (Figure 3b). These curves were plotted using the acoustic events obtained from the AE VALLEN, the stress data obtained from the INSTRON loadcell and the LIMESS strain data.

The first phase of the AE data (Figure 3a) is associated with the occurrence of low energy events starting at the global tensile strain around 0.14% in the warp yarn direction (corresponding to approximately 80 MPa stress), which is designated as the damage initiation strain $\varepsilon_{\min}$ [13]. In the second phase ($\varepsilon_{\min}$ to ε_1 - 0.14 to 0.3%), the rise in the slope of the AE curve is very small, and this phase is related to the occurrence of sporadic cracks which were associated with a low energy release. In the next phase of the AE curve (ε_1 to ε_2 - 0.3 to 0.4%), the slope increases rapidly with the occurrence of low and middle energy acoustic events. The final part of the AE curve (after ε_2) is associated with the continuous events with the high energy release, indicating the critical crack propagation and eventually catastrophic failure of the composite. Once the stress level reached 500 MPa, the AE sensors were removed from the composite specimen to avoid damage to the sensors due to the catastrophic failure of the composite laminate.

Moreover, based on the literature on thermo-plastic composites [18-20], it is observed that the amount of thermal residual stresses accumulated during the manufacturing process can not be neglected. For the carbon-PPS composite plates, thermal stresses were accumulated due to the shrinkage of PPS during the cooling process (micro-mechanical residual stress). In addition, at the micro-level, fibre waviness can influence the residual stresses and hence the failure behavior [20]. At the macro level, unsymmetrical weaving of the 5-harness satin weave fabric causes the warping of composite plates. In general, due to the differences in processing conditions such as layer stacking (internal yarn nesting), different composite plates produced with the same materials tend to exhibit differences in the local warping, which is manifested by the partial relieving of thermal stresses.

In the context of analyzing the variations in thermal stresses in different composite plates, and their influence on the critical strains ($\varepsilon_{\min}, \varepsilon_1, \varepsilon_2$), further investigations were carried out by testing the other batch of carbon-PPS samples made from a different plate. AE tests on the other batch of carbon-PPS samples predicted the damage initiation at an early strain of 0.09% [40 MPa] (Figure 3c). From the AE tests on batch 1 and 2 (Figure 3b, c), it is evident that there is almost a 50% difference in the damage initiation stress due to the variation in thermal residual stresses. Figure 3 (b & c) provides evidence that thermal stresses cause the early damage events with low energy release, which is termed as the damage caused by manufacture induced inhomogeneities. However, in both the cases that are illustrated in Figure 3 (b & c), the rise in event count and the energy release is strongly increased approximately around 200 MPa stress or 0.3-0.4% of average strain.

This is a typical value for the intra-yarn damage onset observed experimentally for many textile composites [8]. Table 3 provides the summary of mechanical properties for the 5-harness satin weave carbon-PPS composite under tension.

3.2. Microscopic analysis of the damage

Microscopic analysis of the composite specimens is a possible technique for evaluating the damage initiation and propagation in the textile laminate. Along with the AE, microscopic analysis allows for the study of the comprehensive damage behaviour of the composite [5, 21]. Quasi-static tensile tests were performed on the polished specimens of the composite laminate, which allowed for the microscopic inspection of the damage initiation and propagation along the thickness direction as well as on the traction free surface of the composite. From the captured microscopic images, apart from the traditional crack counting (crack density) on the polished edges, a new technique is introduced to study the effect of layer stacking on the local damage behavior of the weft yarn. With the help of a satin weave laminate cross section (approximately 8mm) (Figure 4a), details of the damage phenomena starting from the crack initiation to the final failure of the composite is explained in this section.

Due to the sensitivity of the initial damage, up to 100 MPa stress, the load on the INSTRON machine is increased in two steps. After the initial damage, the load is increased with a step size of 100 MPa until the final failure. Damage developed in the 5-harness satin weave under tensile load takes the form of weft yarn cracking, which is

perpendicular to the loading direction (Figure 4a). Moreover, damage initiation occurs at the yarn crimp location and then propagates into the matrix. This type of weft yarn cracking began early in the loading process and almost all weft yarns possess this kind of damage before the final failure of the composite.

To study the effect of local constraints that are posed by the surrounding composite constituents on the weft yarn damage, detailed sequential damage analysis was conducted on the composite specimen. The above mentioned four locations in the laminate (Figure 2a to d) were chosen for this purpose, which can represent different cases where the weft yarn local warping (bending) is allowed or constrained by the adjacent layers [22]. Also, the above mentioned four locations represent the various local fabric geometries that are available in the laminate. By constantly monitoring the weft yarn damage at the above mentioned locations during the loading process, the effects of local yarn constraints on the damage initiation stress and location can be realized.

During the loading process of the composite, initial damage is detected at around the 100MPa stress level on the polished edges of the composite. At these low stress levels, damage occurs at the edges of the weft yarn inside the laminate, in the region where there is no contact between the load carrying warp yarn and the perpendicular weft yarn (Figure 4a). By increasing the stress level from 100 to 400 MPa in three steps, the damage is observed at the nested yarn configurations at various locations in the laminate (Figure 4b). Moreover, the number of cracks between these stress levels can be compared to the event count obtained from AE. By increasing the stress from 400 to 500 MPa, the

next new damage location is observed on the surface of the laminate (Figure 4c). Moreover, 80% of the microscopic images on the surface (top and bottom) of the laminate show the occurrence of intra-yarn damage at the centre of the weft yarn. At this stress level (400-500 MPa), along with the damage on the surface layers, the crack density in the nested yarns inside the laminate is increased at various locations. Finally, between the stress levels of 500-680MPa, the next damage is observed at the edges of the weft yarn, where it is tightly packed by load carrying warp yarns (Figure 4d). Any further loading causes the catastrophic failure of the composite specimen. From the above discussed sequential damage analysis, it can be observed that the local fabric geometry whose local bending is restricted tends to show the initial damage. In contrast, the yarn crimps on the surface layers are relatively more free to deform in the out-of-plane direction, which causes the damage on the surface weft yarns at later stages of the loading.

Besides the qualitative analysis, microscopic images were used for the quantitative analysis as well. The accumulation of transverse matrix cracking in the thickness direction is quantified on the polished edges of the composite. The crack density is measured as a function of the applied stress for the layers of the laminate, by dividing the number of cracks measured in each layer with the laminate gauge length [17]. Figure 5 shows the crack density as a function of applied tensile stress for three composite samples. The microscopic damage analysis described above is in correlation with the AE event pattern. At around the 250 MPa stress level, the event count obtained from AE as well as the crack density tends to increase.

4. Conclusion

A comprehensive damage analysis is conducted on the carbon-PPS 5-harness satin weave composite under uni-axial static tensile load. The damage initiation strain is detected using acoustic emission technique, while the damage locations were detected using microscopic analysis on the polished edges of composite specimens in an interrupted tensile testing process. The analysis of the experimental data leads to the following conclusions.

- Damage initiation in the carbon-PPS satin weave composite varies from 40 to 100MPa stress. The variation of the experimental damage initiation stress in different composite plates can be attributed to the variation in micro level (fibre spacing, intra yarn volume fraction etc) as well as the laminate level (nesting) parameters combined with the thermal residual stresses in the composite.
- From the research output of Le Page et al. [23] and the AE event data obtained from the satin weave composite under tensile load, it can be concluded that the energy release rate and the associated local bending of the satin weave weft yarn increases approximately around 200 MPa global tensile stress.
- From the extensive microscopic analysis of damage in several satin weave laminates, the damage initiation in different layers of the laminate depends on the position of the ply in the laminate. The earliest damage occurs in the inner layers, followed by the transverse crack on the surface weft yarns. This behaviour is related to the constraints posed by the neighbouring layers on the local ply.

- Initial transverse cracks tend to be located near the edges of the weft yarns cross-section rather than the centre.
- The above conclusions are entirely supported by the work of Ivanov. [7], in which the author reported that the meso stress distribution, and crack density is different for inner and outer layers of the laminate. Moreover, meso stress distribution depends upon the stacking sequence, ply shift and the number of plies in the laminate [8].

The damage phenomena discussed above focus mainly on the qualitative damage behaviour of the satin weave composite. In part II of this series, deterministic numerical simulations provide overall insight into the mechanics of damage and the local stress behaviour of the yarns. This cannot be determined using the conventional experimental techniques.

ACKNOWLEDGEMENTS

The authors would like to acknowledge the FWO - Vlaanderen for the financial support provided through the project G.0233.06H. Assistance from the laboratory staff at the department of MTM – Kris van der Staey and Johan Vanhuist is gratefully acknowledged. The authors also express their gratitude to ‘Ten Cate’ for supplying the composite plates.

REFERENCES

[1]. Ivanov, D.S., et al., *Failure Analysis of Triaxial Braided Composite.* Composites Science and Technology. **In Press, Accepted Manuscript**.

[2]. Dzenis, Y.A. and J. Qian, *Analysis of microdamage evolution histories in composites.* International Journal of Solids and Structures, 2001. **38**(10-13): p. 1831-1854.

[3]. Koissin, V. and D.S. Ivanov, *Fibre distribution inside yarns of textile composite: geometrical and FE modelling.* Proceedings of the 8th International Conference on Textile Composites (TexComp-8).Nottingham: CD edition, 2006.

[4]. Kurashiki, T., et al., *A numerical simulation of damage development for laminated woven composites* ECCM-13 Proceedings, 2008.

[5]. John, S., I. Herszberg, and F. Coman, *Longitudinal and transverse damage taxonomy in woven composite components.* Composites Part B: Engineering, 2001. **32**(8): p. 659-668.

[6]. Anzelotti, G., G. Nicoletto, and E. Riva, *Mesomechanic strain analysis of twill-weave composite lamina under unidirectional in-plane tension.* Composites Part A: Applied Science and Manufacturing, 2008. **39**(8): p. 1294-1301.

[7]. Ivanov, d.S., *Damage analysis in textile composites.* PhD Thesis; KU Leuven - Faculty of Engineering, May 2009.

[8]. Ivanov, D.S., et al., *Stress distribution in outer and inner plies of textile laminates and novel boundary conditions for unit cell analysis.* Composites Part A: Applied Science and Manufacturing. **In Press, Accepted Manuscript**.

[9]. Mattsson, D., R. Joffe, and J. Varna, *Damage in NCF composites under tension: Effect of layer stacking sequence.* Engineering Fracture Mechanics, 2008. **75**(9): p. 2666-2682.

[10]. Morscher, G.N., *Modal acoustic emission of damage accumulation in a woven SiC/SiC composite.* Composites Science and Technology, 1999. **59**(5): p. 687-697.

[11]. Giordano, M., et al., *An acoustic-emission characterization of the failure modes in polymer-composite materials.* Composites Science and Technology, 1998. **58**(12): p. 1923-1928.

[12]. Ivanov, D., et al., *Strain mapping analysis of textile composites.* Optics and Lasers in Engineering. **In Press, Corrected Proof**.

[13]. Lomov, S.V., et al., *A comparative study of tensile properties of non-crimp 3d orthogonal weave and multi-layer plain weave e-glass composites. Part 1: Materials, Methods and Principal Results.* Composites Part A: Applied Science and Manufacturing. **In Press, Accepted Manuscript**.

[14]. Ivanov, D.S., et al., *A comparative study of tensile properties of non-crimp 3D orthogonal weave and multi-layer plain weave E-glass composites. Part 2: Comprehensive experimental results.* Composites Part A: Applied Science and Manufacturing. **In Press, Corrected Proof**.

[15]. Vallen, S.G.-. *AE Testing (AT) Fundamentals - Equipment - Data Analysis (Overview).*
[16]. Searles, K., J. McCarthy, and M. Kumosa, *An image analysis technique for evaluating internal damage in graphite-fabric/polyimide composites.* Composites Science and Technology, 1998. **58**(10): p. 1607-1619.
[17]. Gao, F., et al., *Damage accumulation in woven-fabric CFRP laminates under tensile loading: Part 1. Observations of damage accumulation.* Composites Science and Technology, 1999. **59**(1): p. 123-136.
[18]. Parlevliet, P.P., H.E.N. Bersee, and A. Beukers, *Residual stresses in thermoplastic composites--A study of the literature--Part I: Formation of residual stresses.* Composites Part A: Applied Science and Manufacturing, 2006. **37**(11): p. 1847-1857.
[19]. Parlevliet, P.P., H.E.N. Bersee, and A. Beukers, *Residual stresses in thermoplastic composites - a study of the literature. Part III: Effects of thermal residual stresses.* Composites Part A: Applied Science and Manufacturing, 2007. **38**(6): p. 1581-1596.
[20]. Parlevliet, P.P., H.E.N. Bersee, and A. Beukers, *Residual stresses in thermoplastic composites--A study of the literature--Part II: Experimental techniques.* Composites Part A: Applied Science and Manufacturing, 2007. **38**(3): p. 651-665.
[21]. Lomov, S.V., et al., *Experimental methodology of study of damage initiation and development in textile composites in uniaxial tensile test.* Composites Science and Technology, 2008. **68**(12): p. 2340-2349.
[22]. Ito, M. and T.-W. Chou, *Elastic moduli and stress field of plain-weave composites under tensile loading.* Composites Science and Technology, 1997. **57**(7): p. 787-800.
[23]. Le Page, B.H., et al., *Finite element simulation of woven fabric composites.* Composites Part A: Applied Science and Manufacturing, 2004. **35**(7-8): p. 861-872.
[24]. De Baere, I., *Experimental and Numerical Study of Different Setups for Conducting and Monitoring Fatigue Experiments of Fibre-Reinforced Thermoplastics.* PhD Thesis, Gent university, 2008.

Table 1. Parameters of the AE (Acoustic Emission) equipment.

Software	*Vallen AMSY-5*
Amplifiers	*Vallen AEP4*
Amplification, dB	*34*
Discrimination time, ms	*0.4*
Rearm time, ms	*3.2*
Range, MHz	*0.025..1.6*
Sample rate, MHz	*5*
Sensors	*Digital wave 1025*
Sensor diameter, cm	*0.93*
Threshold, dB	*35*

Table 2. Satin weave carbon/PPS composite information.

Carbon fibre type	*T300JB*
TEX, (g/km)	*198*
End/Pick count, yarns per 10 cm	*70*
Yarn filament count	*3000*
Filament diameter, (mm)	*0.007*
Carbon fibre density, (g/cm^3)	*1.75*
Fabric areal density, (g/m^2)	*285*
Overall fibre volume fraction	*$50 \pm 3\%$*

Table 3. Experimental mechanical properties of the carbon-PPS satin weave composite.

	Warp direction	*Weft direction*
Young's modulus, GPa	*57 ± 1*	*57 ± 1*
In-plane Poisson's ratio ν_{12}	0.05 ± 0.02	
In-plane shear modulus G_{12}, GPa[24]	4175	
Strength, MPa	*734*	*754*
Ultimate strain, %	*1.1 ± 0.1*	*1.1 ± 0.1*
Damage initiation $\varepsilon_{\min}$, %	*0.09 -0.2*	*-NA-*
First damage threshold ε_1, %	*0.3-0.35*	*-NA-*
Second damage threshold ε_2, %	*0.4-0.45*	*-NA-*

Weft yarn damage at the laminate level

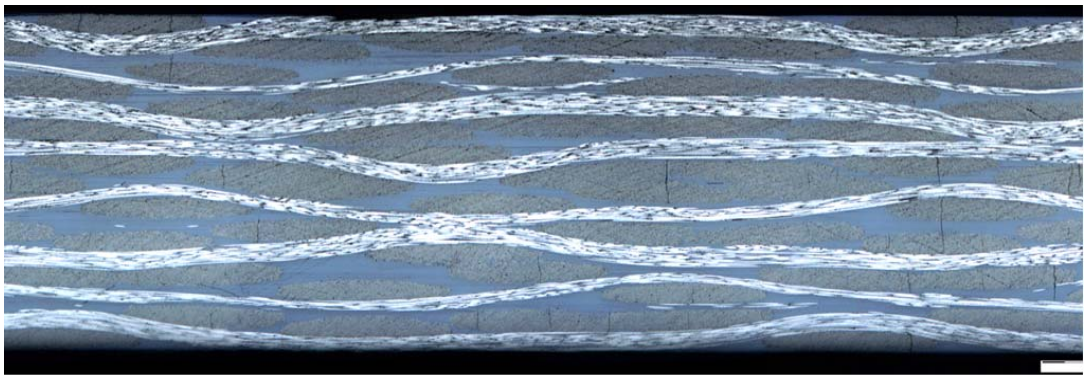

Ply level– Weft yarn damage on the surface layer (at the weft yarn centre)

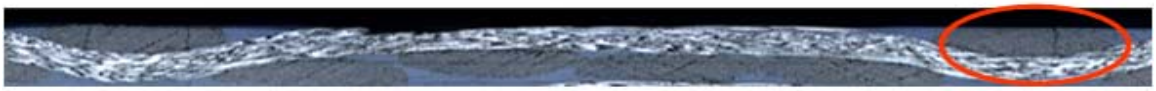

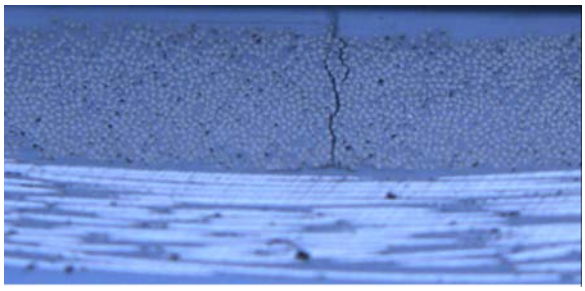

Ply level – Weft yarn damage at nested yarn configuration (at the edge of the weft yarn)

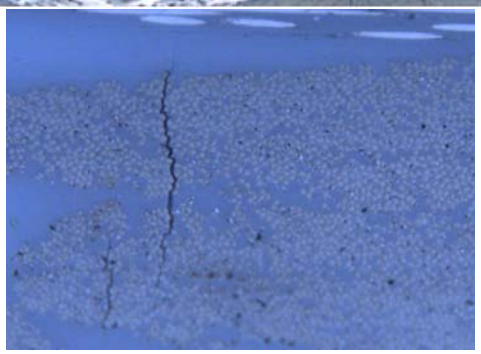

Micro level- fibre matrix debonding in the weft yarn

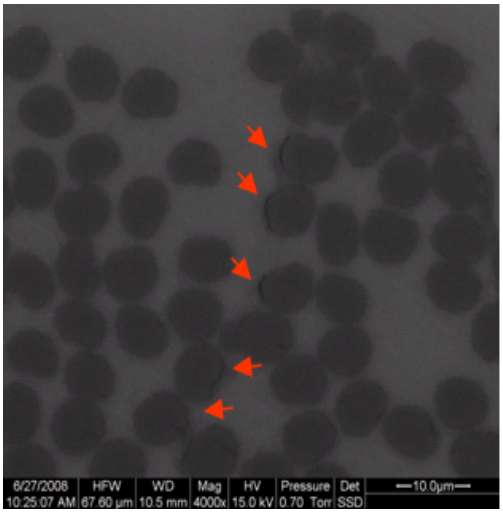

Figure 1. *Schematic representation of the damage at various levels in a satin weave carbon-pps thermoplastic composite.*

a)

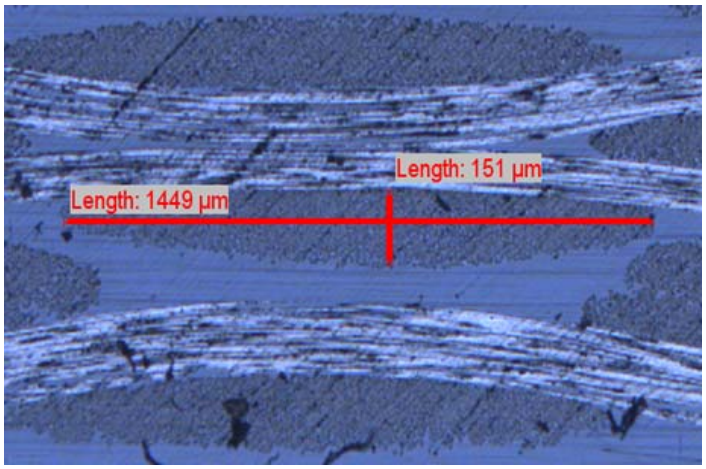

Major dia =1499 μm
Minor dia =151 μm

b)

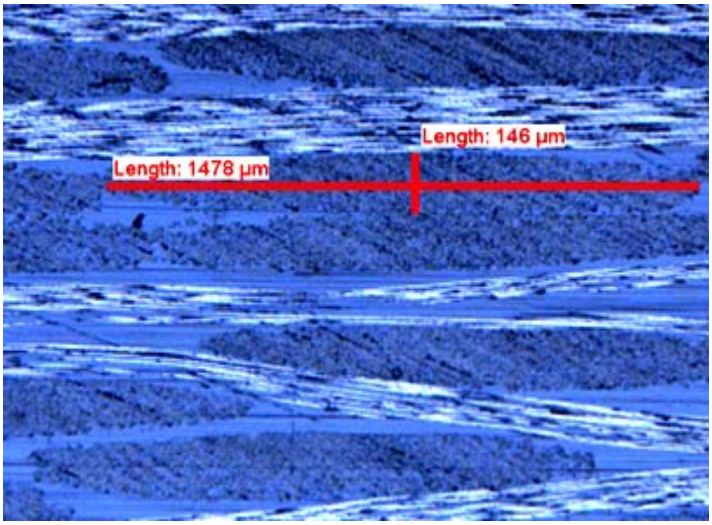

Major dia =1478 μm
Minor dia =146 μm

c)

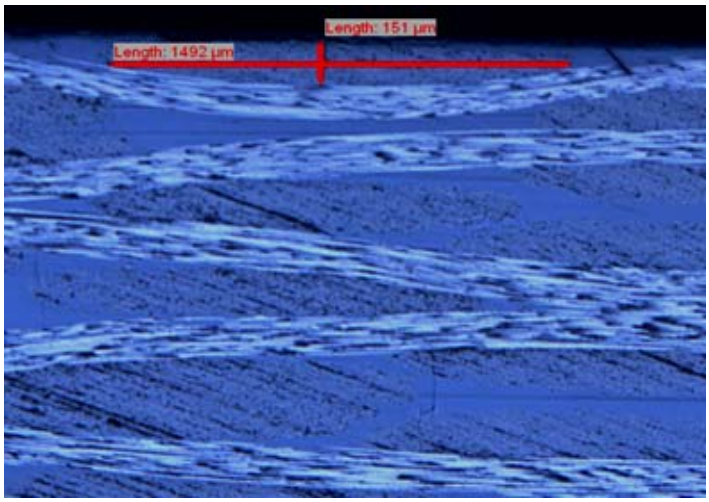

Major dia =1492 μm

Minor dia =151 μm

d)

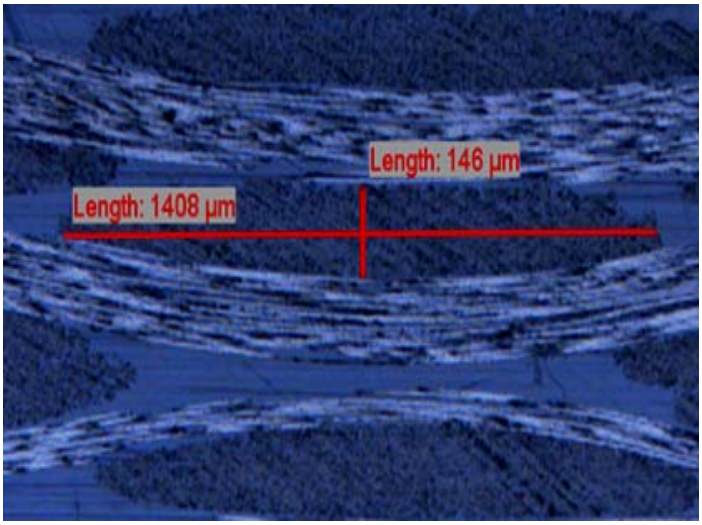

Major dia =1408 μm

Minor dia =146 μm

Figure 2. Weft yarn dimensions measured at a) yarn in the resin rich region; b) nested yarns; c) surface of the laminate; d) tightly packed by warp yarns.

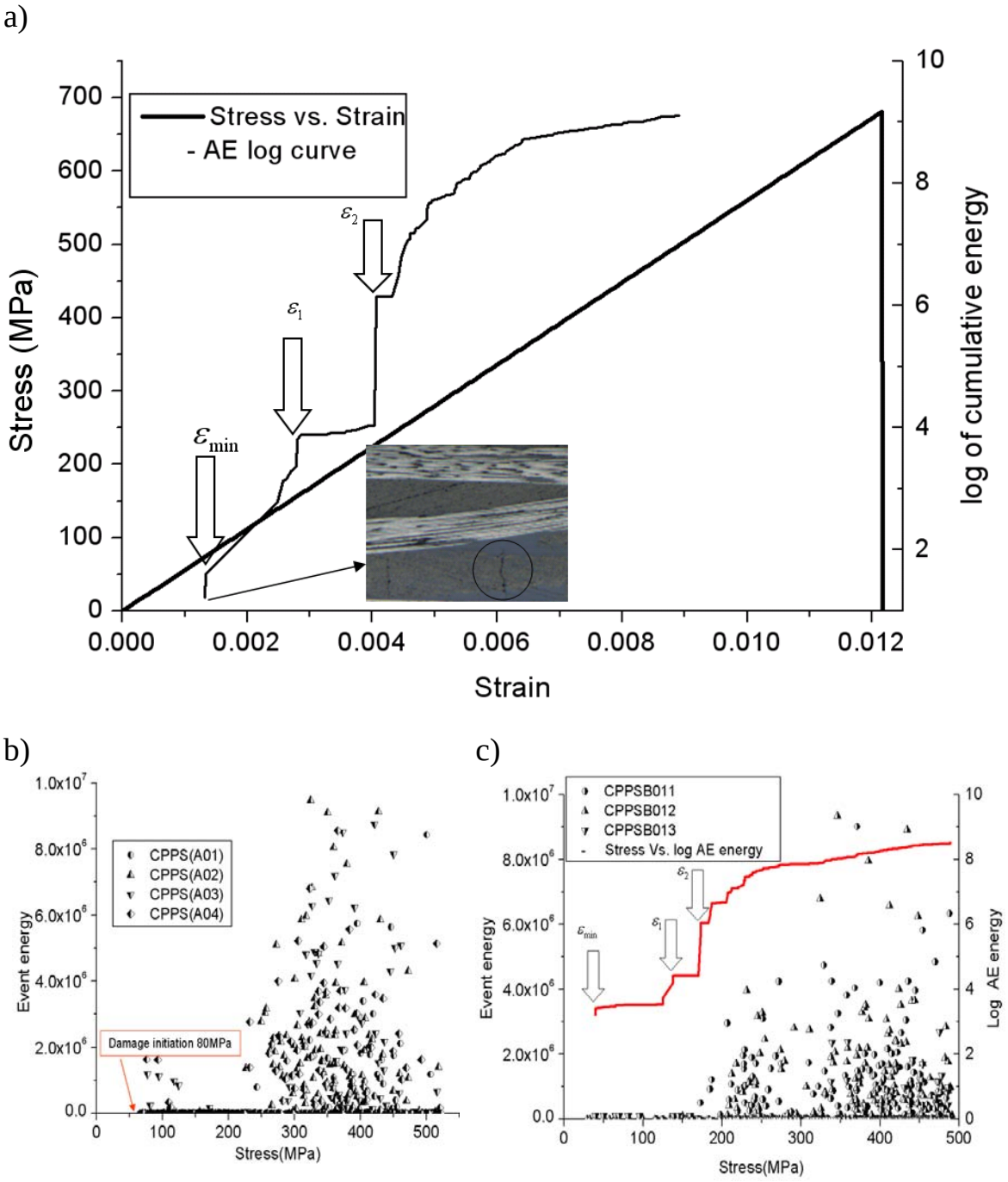

Figure 3. *a) Stress vs. strain and strain vs. AE registration curve (test1); b) AE event pattern (batch 1); c) AE event pattern (batch 2).*

a)

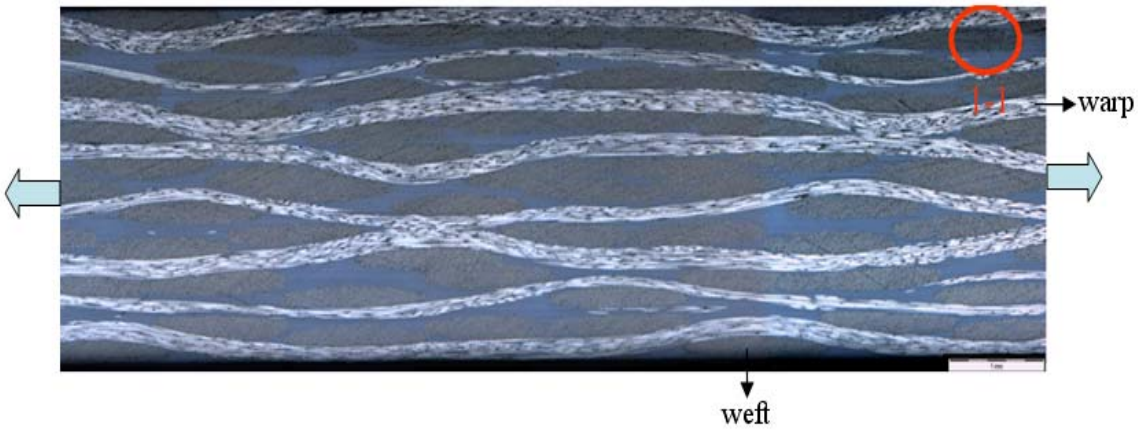

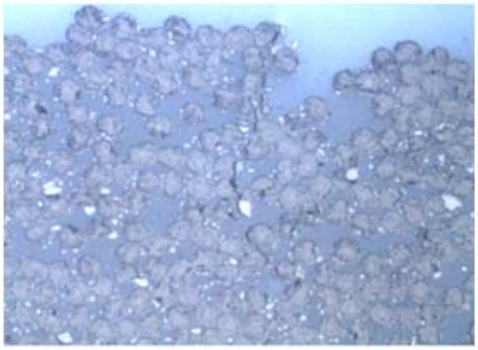

Damage 1-1

b)

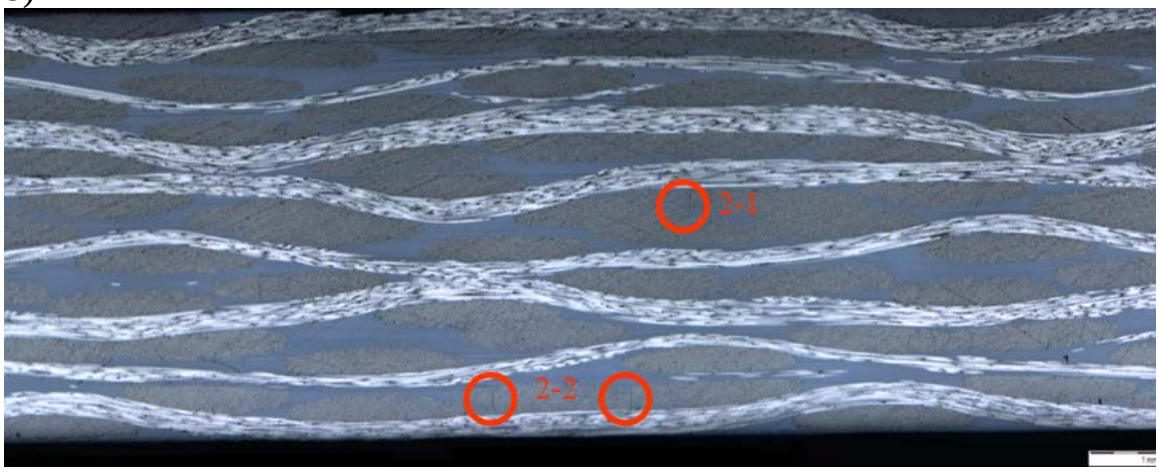

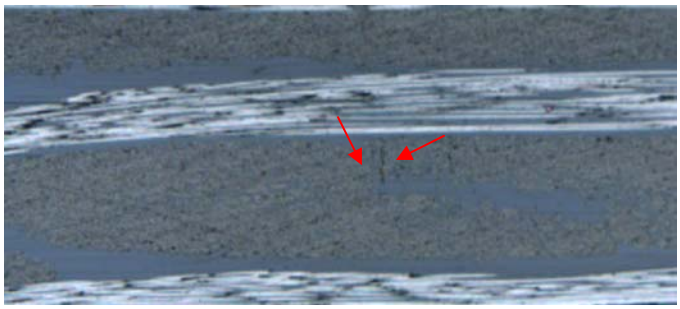

Damage location at 2-1(nested yarn)

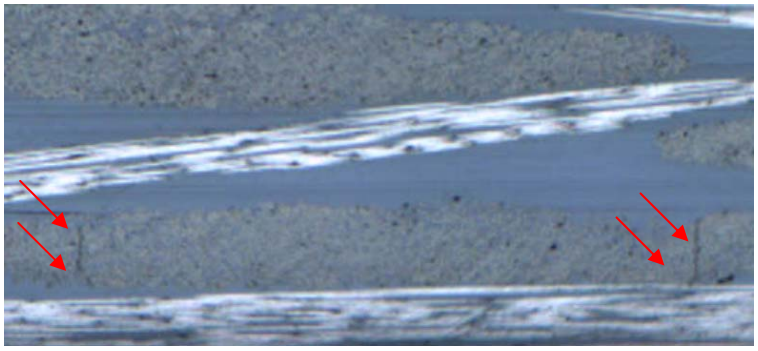

Damage location at 2-2 (nested yarn)

c)

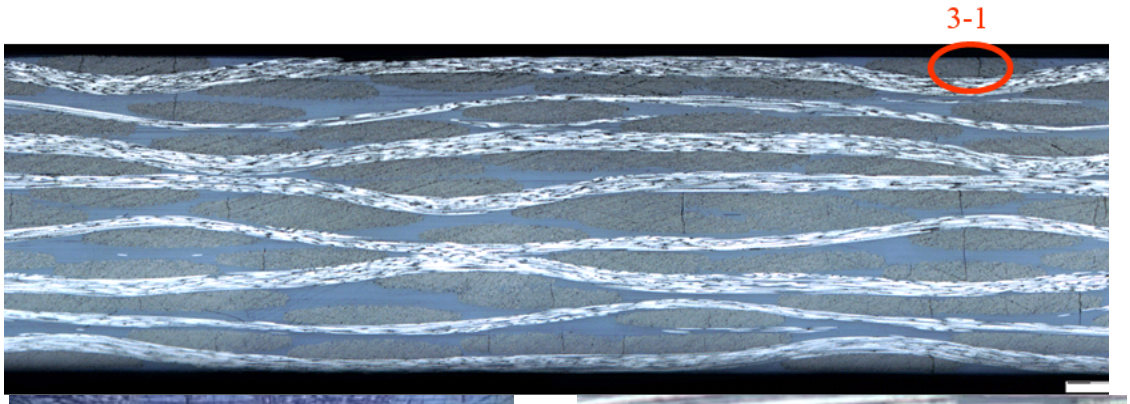

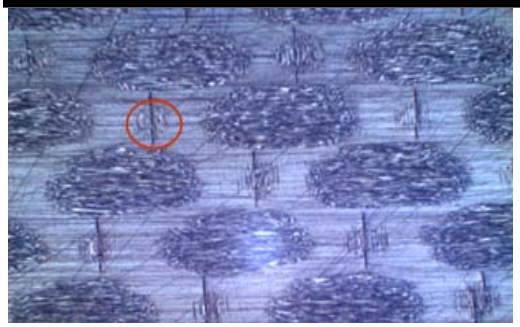

Damage location 3-1 (Surface yarn) top view

Damage location 3-1(Surface yarn) side view

d)

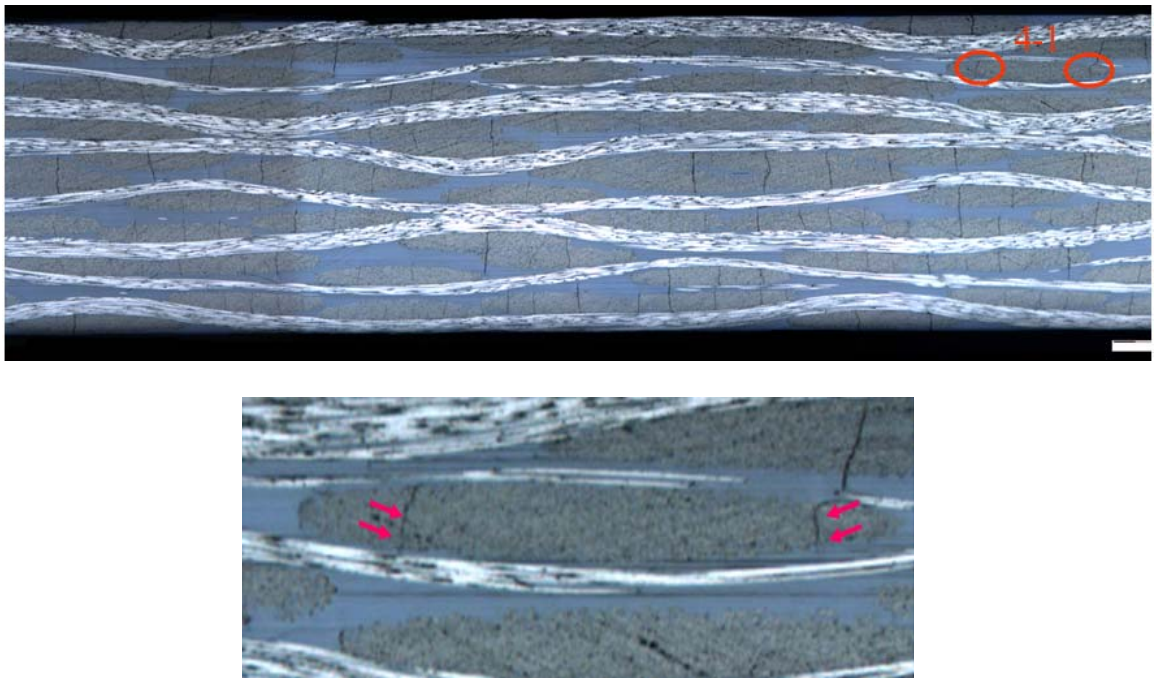

Damage at location 4-1

Figure 4. *Microscopic sequential damage analysis : a) laminate at100MPa tensile stress; b) tensile stress between 100 - 400 MPa; c) tensile stress between 400 – 500 MPa; d) tensile stress between 500 – 680 MPa (Size bar is 1mm).*

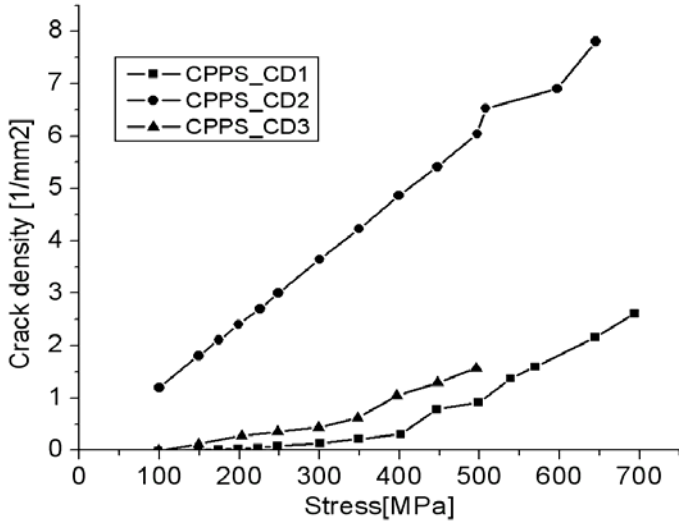

Figure 5. *Crack density as a function of applied tensile stress.*